Journal of Colloid and Interface Science 524 (2018) 279–288

Contents lists available at ScienceDirect

Journal of Colloid and Interface Science

journal homepage: www.elsevier.com/locate/jcis

Regular Article

Microstructural characteristics of surfactant assembly into a gel-like mesophase for application as an oil spill dispersant

Olasehinde Owoseni [a], Yueheng Zhang [a], Marzhana Omarova [a], Xin Li [b], Jyotsana Lal [b], Gary L. McPherson [c], Srinivasa R. Raghavan [d], Arijit Bose [e], Vijay T. John [a,*]

[a] Department of Chemical and Biomolecular Engineering, Tulane University, New Orleans, LA 70118, USA
[b] Louisiana Consortium for Neutron Scattering, Louisiana State University, Baton Rouge, LA 70803, USA
[c] Department of Chemistry, Tulane University, New Orleans, LA 70118, USA
[d] Department of Chemical and Biomolecular Engineering, University of Maryland, College Park, MD 20742, USA
[e] Department of Chemical Engineering, University of Rhode Island, Kingston, RI 02881, USA

GRAPHICAL ABSTRACT

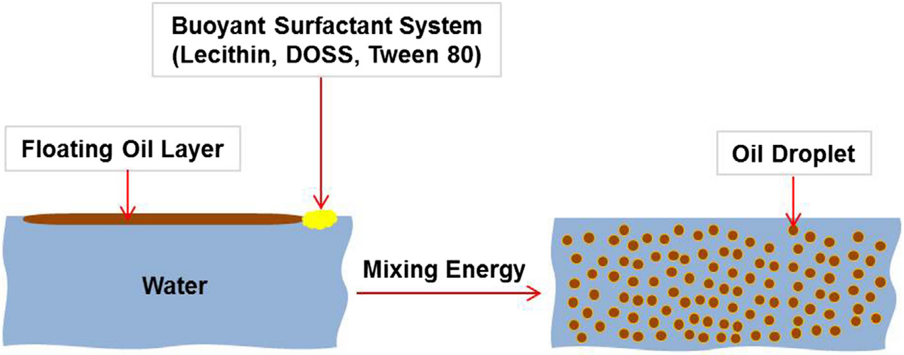

ARTICLE INFO

Article history:
Received 6 January 2018
Revised 24 March 2018
Accepted 26 March 2018
Available online 6 April 2018

Keywords:
Surfactant
Gel-like mesophase
Microstructure
Emulsions
Oil spills

ABSTRACT

Hypothesis: Polyoxyethylene (20) sorbitan monooleate (Tween 80) can be incorporated into the gel-like phase formed by L-α-phosphatidylcholine (PC) and dioctyl sulfosuccinate sodium salt (DOSS) for potential application as a gel-like dispersant for oil spill treatment. Such gel-like dispersants offer advantages over existing liquid dispersants for mitigating oil spill impacts.

Experiments: Crude oil-in-saline water emulsions stabilized by the surfactant system were characterized by optical microscopy and turbidity measurements while interfacial tensions were measured by the spinning drop and pendant drop techniques. The microstructure of the gel-like surfactant mesophase was elucidated using small angle neutron scattering (SANS), cryo scanning electron microscopy (cryo-SEM), and ^{31}P nuclear magnetic resonance (NMR) spectroscopy.

Findings: The gel-like phase consisting of PC, DOSS and Tween 80 is positively buoyant on water and breaks down on contact with floating crude oil layers to release the surfactant components. The surfactant mixture effectively lowers the crude oil-saline water interfacial tension to the 10^{-2} mN/m range, producing stable crude oil-in-saline water emulsions with an average droplet size of about 7.81 μm. Analysis of SANS, cryo-SEM and NMR spectroscopy data reveals that the gel-like mesophase has a lamellar microstructure that transition from rolled lamellar sheets to onion-like, multilamellar structures with increasing Tween 80 content.

---

* Corresponding author.
E-mail address: vj@tulane.edu (V.T. John).

https://doi.org/10.1016/j.jcis.2018.03.089

1. Introduction

Amphiphilic molecules assemble into a range of aggregates such as micelles, reverse micelles, fibrils, wormlike micelles, and vesicles [1–3]. At high concentrations, surfactant and lipids form mesophases which can be arrays of cylinders (hexagonal or nematic), stacks of bilayers (lamellar, smectic, liposome) or a complex three dimensional network of interconnected structures (bicontinuous, tricontinuous) [1].

In the treatment of oil spills, surfactant systems known as dispersants are applied to lower the oil-water interfacial tension and facilitate oil dispersion for subsequent biodegradation [2,4–6]. Traditional dispersants are liquid formulations of surfactant such as DOSS (dioctyl sulfosuccinate sodium salt), Tween 80 (polyoxyethylene (20) sorbitan monooleate) and Span 80 (sorbitan monooleate) in organic solvents, typically propylene glycol and petroleum distillates to provide single phase compatibility with the oil and water soluble surfactants in the formulation [7]. The DOSS component, which is anionic, has been reported to stabilize the oil-water interface formed during the breakup of dispersant treated oil [8], while the nonionic surfactant components allows the attainment and retention of low interfacial tensions [7,8]. The synergy of the surfactant components facilitates the formation of stable emulsions that are not readily obtained with a single surfactant [7,9].

A key challenge to the effective use of existing liquid dispersants in the treatment of oil spills is that the dispersants suffer from spray drift and gets washed off by ocean currents, especially when applied onto heavy or weathered oils [7,10,11]. To overcome the current limitations of existing liquid dispersants, research efforts have advanced the design of alternative dispersant systems including gel-like dispersants [7,10–14]. Key beneficial characteristics of gel type dispersants over traditional liquid dispersants include (a) close adherence to the spill oils without being washed off (b) buoyancy for extended periods allowing more contact with oil (c) high surfactant concentrations and (d) possibility of the gel-like dispersants providing some degree of visible feedback to oil spill responders [10].

Our research described in this article is based on the development of a gel type dispersant. In recent collaborative work with the Raghavan laboratory, a liquid formulation of two food grade amphiphiles, Lecithin and Tween 80, dissolved in ethanol was found to be as effective as the commercial dispersant, Corexit 9500, in stabilizing oil-in-water emulsions [12]. The study showed that, while Lecithin or Tween 80 alone were ineffective in stabilizing crude oil-in-saline water emulsions, blends of Lecithin and Tween 80 improved the stability of these emulsions [12]. It should be noted that the major component in the Lecithin used in the above study is the innocuous double-tailed phospholipid, L-α-phosphatidylcholine (PC). The conceptual aspects of this work was that the large headgroups of Tween 80 provide steric repulsion to droplet coalescence while the oil soluble PC as a double tailed replacement for DOSS helped stabilize the interface through extended retention in the oil phase. The synergy between PC and Tween 80 helped reduce interfacial tension to values of 10^{-1} mN/m or lower to facilitate formation of oil droplets.

However, the PC+Tween 80 system is not in a gel phase and is difficult to formulate into a gel phase. We have used earlier results from our laboratory on PC+DOSS systems to attempt to formulate gel phase dispersants. Thus, in our earlier work, we found that the addition of water to a micellar solution of PC and DOSS in an organic solvent leads to the formation of a gel-like mesophase that can incorporate very high water content [15–17]. The synergy of PC and DOSS is necessary to form the gel-like mesophase as the system breaks downs and phase separates at much lower water contents for DOSS or PC alone [15].

Our objective here is to exploit the self-assembly of PC, DOSS and Tween 80 into a gel-like phase for potential application as a buoyant gel dispersant for oil spill remediation. In this paper, we demonstrate how the inclusion of Tween 80 into the gel-like phase significantly enhances the stabilization of crude oil-in-saline water emulsions. The gel-like surfactant mesophase is buoyant on water and the mechanism for dispersing floating crude oil layers is demonstrated. The microstructure of the gel-like surfactant phase is further characterized using Small Angle Neutron Scattering (SANS), ^{31}P Nuclear Magnetic Resonance (NMR) Spectroscopy and Cryogenic Scanning Electron Microscopy (cryo-SEM). The systematic introduction of the nonionic surfactant, Tween 80, allows the elucidation of the transitions in the gel microstructure with Tween 80 content. Thus, we show that these gel-like surfactant mesophases constitute a new class of effective dispersants for the treatment of oil spills. The chemical structures of PC, DOSS and Tween 80 are presented in the supporting information.

2. Experimental

2.1. Materials

Dioctyl sulfosuccinate sodium salt (DOSS, 98% purity), polyoxyethylene (20) sorbitan monooleate (Tween 80), deuterium dimethyl sulfoxide (DMSO-d_6, 99.9%) and hexadecane were purchased from Sigma Aldrich. L-α-Phosphatidylcholine (95%) extracted from soybeans was purchased from Avanti Polar Lipids, Inc. Deuterium oxide (D_2O, 99.9%) was obtained from Cambridge Isotopes Laboratory. Deionized (DI) water, produced from an Elga water purification system (Medica DV25), with resistivity of 18.2 MΩ cm was used in all experiments. 0.6 M sodium chloride (Certified ACS grade, Fisher Scientific) solution in deionized water was used as a substitute for seawater. Louisiana sweet crude oil with a viscosity of 0.01 Pa s and specific gravity 0.85 at 15 °C was obtained from British Petroleum's Macondo prospect (SOB-20100617032) [7]. All chemicals were used as received.

2.2. Synthesis of Gel-Like surfactant mesophase

In the preparation of the gel-like mesophases, the PC to DOSS molar ratio was first varied from 0 to 1 with the total surfactant concentration fixed at 1.26 M in hexadecane. The appropriate mass of each surfactant used in preparing the samples are summarized in Table 1. The surfactant components were dissolved into 5 ml of hexadecane by intermittent sonication in a water bath and magnetic stirring at 50 °C. Water was then gradually added into the system in 0.5 ml increments. The surfactant system was mixed on a vortex mixer (Thermolyne Maxi Mix II) after each addition of water until the mixture became homogeneous. As shown in Table 1, DOSS alone does not form a gel at these compositions. A gel-like mesophase forms above a threshold molar ratio of PC to DOSS of 2:5.

In this work, we focus on the system prepared with equimolar PC to DOSS content to maximize the use of the food grade phospholipid, PC. Systems with higher amounts of PC (greater than 2.39 g) are not readily dispersible in 5 ml of the organic solvent and are not reported here. For the equimolar PC (2.39 g) and DOSS (1.40 g) micellar solution in 5 ml hexadecane, the addition of 2.5 ml of water marks the onset of gelation. Increasing Tween 80 amounts of 0.625 g, 1.25 g, 2.5 g, 3.0 g and 3.75 g were then incorporated into the gel phase prepared with PC and DOSS. Tween 80 (Sigma Aldrich) was added in 0.25 g increments followed by vortex mixing until the mixture became homogeneous (representative photograph in Fig. 1). The gel-like surfactant system flows on

Table 1
Sample compositions prepared at varying PC to DOSS ratio.

Molar ratio of PC to DOSS	Mass of Surfactant (g)		Surfactant Concentration in hexadecane (M)			Formation of Gel-like Phase (Yes/No)
	PC	DOSS	PC	DOSS	PC + DOSS	
0.00	0.00	2.80	0.00	1.26	1.26	No
0.14	0.60	2.45	0.16	1.10	1.26	No
0.20	0.80	2.33	0.21	1.05	1.26	No
0.33	1.19	2.10	0.32	0.95	1.26	No
0.40	1.36	2.00	0.36	0.90	1.26	Yes
0.50	1.59	1.87	0.42	0.84	1.26	Yes
0.60	1.79	1.75	0.47	0.79	1.26	Yes
0.67	1.91	1.68	0.50	0.76	1.26	Yes
0.80	2.12	1.56	0.56	0.70	1.26	Yes
1.00	2.39	1.40	0.63	0.63	1.26	Yes

tilting the vial at Tween 80 loadings greater than 3.75 g indicating a breakdown of the system.

2.3. Oil emulsification and stability characterization

The gel-like surfactant system was mixed with crude oil by vortex mixing and sonication. The mixture was then added to a 20 ml vial containing saline water followed by vortex mixing (Thermolyne Maxi Mix II, 37 W) for 1 min at 3000 rpm. Emulsions were imaged on a Leica DMI REZ optical microscope and the images were analyzed to obtain the droplet sizes. In the turbidimetric experiments the oil to water volume ratio was 0.003. An aliquot of the emulsion (~1.5 ml) was quickly transferred to a quartz cuvette (path length = 10 mm). The percentage light transmittance through the emulsion was then measured as a function of time using a UV–vis Spectrophotometer (Shimadzu UV-1700) at a wavelength of 400 nm [18]. The UV Probe software (version 2.32) was used for data analysis.

2.4. Interfacial tension measurements

Interfacial tensions were measured by the spinning drop and pendant drop techniques to span the range of crude oil-saline water interfacial tensions. For low interfacial tensions (≤2 mN/m) of the dispersant-oil mixtures, the interfacial tension was measured using the spinning drop technique (Grace Instruments model M6500 tensiometer). The tensiometer uses a rotating capillary of 2 mm inner diameter with total volume of 0.292 cm^3. The capillary was first filled with saline water and 0.001 cm^3 of the surfactant-oil mixtures were then injected using a micro syringe to create a small oil drop in the external saline water phase. The capillary tube was sealed and then rotated at a velocity in the range of 5000–6000 rpm. The capillary tube temperature was maintained at 25 °C by a cold water circulation around the tube.

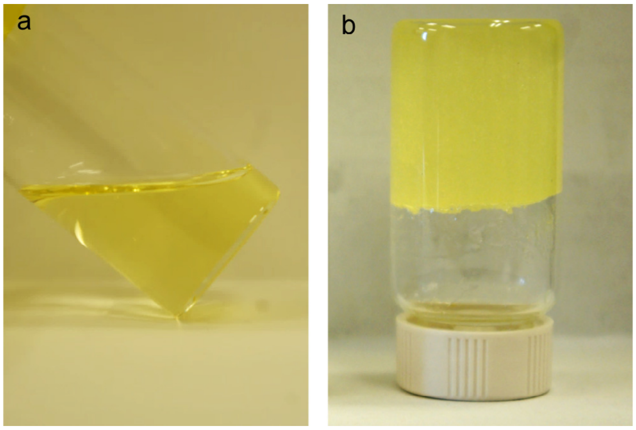

Fig. 1. (a) Photograph of the starting surfactant solution (PC and DOSS) and (b) representative photograph of gel-like system on addition of water and Tween 80.

Interfacial tensions were calculated using the Vonnegut's formula [19,20]:

$$\gamma = \frac{\Delta\rho\omega^2 R^3}{4} \qquad (1)$$

where γ (mN m^{-1}) is the crude oil-saline water interfacial tension, $\Delta\rho$ (g cm^{-3}) is the density difference between the drop and the surrounding fluid, ω (rad s^{-1}) is the angular velocity, and R (cm) is the drop radius measured using an optical microscope fitted with a digital output. The Vonnegut's formula is valid within 0.1% accuracy when the length of the oil drop exceeds four times its diameter [19]. Systems with high interfacial tensions that do not satisfy this condition were measured by the pendant drop method using a standard goniometer (ramé-hart Model 250) and the analysis was carried out using the DROPimage Advanced Software.

2.5. SANS data collection and reduction

The microstructure of the gel-like surfactant system was characterized using Small Angle Neutron Scattering (SANS). SANS experiments were carried out at the extended-Q range small-angle neutron scattering (EQ-SANS) instrument of the Spallation Neutron Source at Oak Ridge National Laboratory. Samples were prepared with D_2O (2.5 ml) as the aqueous phase to provide contrast for the aqueous domains. The samples were loaded into 2 mm path-length quartz cells (Hellma, Germany) and the SANS measurements were made at 25 °C. The scattering angle (θ) is related to the neutron wavelength (λ) and scattering vector (q) by the equation [21]:

$$q = \frac{4\pi}{\lambda}\sin\left(\frac{\theta}{2}\right) \qquad (2)$$

The time-of-flight EQ-SANS instrument was operated in 60 Hz mode with neutron band wavelength (λ) range of 2.5 Å–6.1 Å. This provided an effective q-range of ~0.009–0.44 Å^{-1}. The sample-to-detector distance was 4 m.

Standard SANS data reduction procedures were implemented in MantidPlot [22]. The data were corrected for instrument dark current (cosmic radiation and electronic noise), detector sensitivity, background, incident beam normalization and sample transmission. A calibrated standard, Porasil B, was used to convert the data into absolute intensity units (1/cm) [23]. Reduced data were azimuthally averaged using MantidPlot to produce profiles of scattering intensity, *I(q)* as a function of the scattering vector, *q*.

2.6. Cryo-Field emission scanning electron microscopy imaging

Cryo-SEM imaging of the gel-like surfactant system was performed using a Hitachi S-4800 field emission Scanning Electron Microscope operated at a voltage of 3 kV and a working distance of 9 mm. The samples were transferred into rivets mounted onto the cryo-SEM sample holder. The samples were then plunged into slushed liquid nitrogen to freeze the sample. This was followed by fracturing at −130 °C using a flat-edge cold knife and sublimation of the solvent at −95 °C for 5 min. The temperature was lowered back to −130 °C and the sample was then sputtered with a gold–palladium composite at 10 mA for 88 s before imaging.

2.7. ^{31}P nuclear magnetic resonance (NMR) spectroscopy

NMR spectra were acquired using a Bruker 500 MHz NMR spectrometer operating at 25 °C. Samples of gel-like surfactant mesophases were held in coaxial NMR tubes. In a typical experiment, about 500 µL of the gel-like surfactant systems was first transferred into an 8 cm long, 5 mm diameter NMR tube. The sample was transferred with the aid of a 1 ml syringe fitted with a 15 cm long needle with 2 mm outer diameter and 1.5 mm internal diameter. A 2.5 mm diameter NMR tube containing DMSO lock agent was inserted into the 5 mm NMR tube containing the sample. The tubes were sealed and NMR spectra were acquired after a 5 min equilibration time.

2.8. Rheological measurements

Rheological properties (under steady as well as oscillatory shear) of the gel-like surfactant systems were measured at room temperature on a TA instruments AR-2000 rheometer. A cone and plate geometry, with a cone angle of 1° and a diameter of 40 mm, was used. A solvent trap was used to mitigate solvent loss from the sample. For the oscillatory shear measurements, a constant strain of 0.5% was used.

3. Results and discussion

3.1. Crude oil emulsification and stabilization mechanisms

The compositions of the gel-like surfactant mesophases with different Tween 80 loadings are presented in Table 2. For brevity, the systems are simply referenced in terms of the percentage weight of the Tween 80 component. The oil emulsification ability of the PC-DOSS system without Tween 80 is first characterized. Fig. 2a shows that the mixture of PC and DOSS leads to unstable emulsions, with the crude oil phase completely resurfacing within 10 min. Incorporation of Tween 80 into the DOSS-PC system results in a significant enhancement in emulsion stability over time (Fig. 2a).

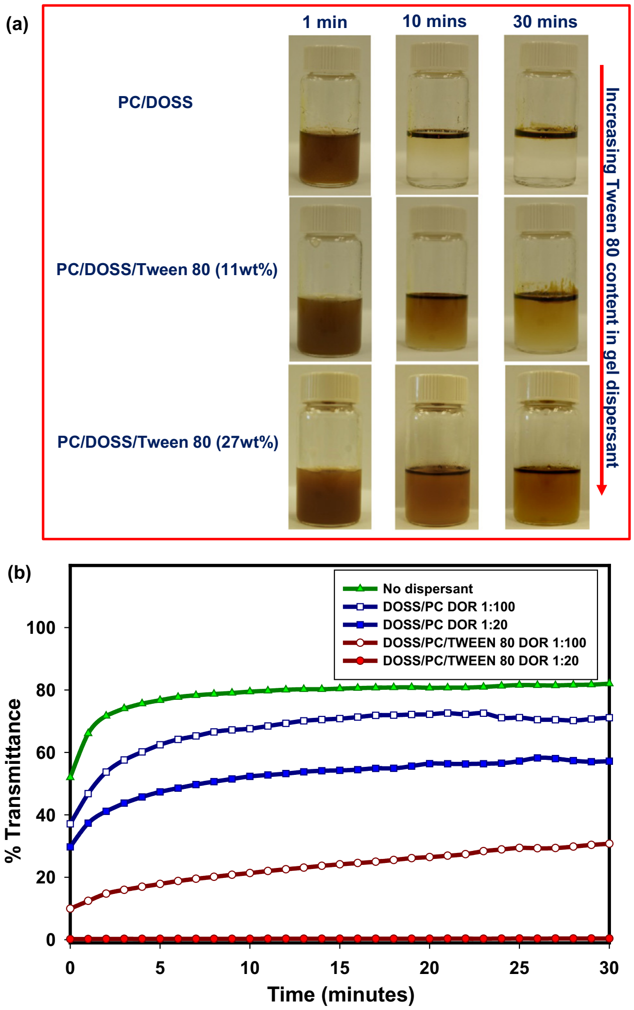

Fig. 2. (a) Stability of crude oil-in-saline water emulsions prepared with PC/DOSS/Tween 80 gel-like system with increasing Tween 80 content. Surfactant system to oil mass ratio is 1:20 and oil to saline water ratio is 1:100. The systems were prepared with equimolar amounts of PC and DOSS in hexadecane. (b) Turbidity of crude oil-in-saline water emulsions as a function of time and dispersant to oil mass ratio (DOR). DOR is the mass ratio of the gel-like surfactant system (dispersant) to the oil phase. The DOSS/PC/Tween 80 system has a Tween 80 content of 27 wt%.

Turbidity of emulsions were measured as a function of time to quantitatively characterize the stability [18]. In Fig. 2b, the mass ratio of the gel-like surfactant system (dispersant) to the crude oil is referred to as the dispersant to oil ratio (DOR). The transmittance is highest for the crude oil-saline water mixture without dispersant, indicating that the dispersed oil rapidly rises (creams) to the surface. This rapid creaming is driven by the spontaneous tendency of the system to minimize the interfacial area between the

Table 2
Composition of gel-like surfactant system.[a]

Mass of Tween 80 in gel-like system (g)	$\alpha_{\text{Tween 80}}$	α_{PC}	α_{DOSS}	α_s	α_w	α_o
0	0	24	14	37	25	38
0.625	6	22	13	41	23	36
1.25	11	21	12	44	22	34
2.50	20	19	11	50	20	30
3.00	23	18	11	52	19	29
3.75	27	17	10	54	18	28

[a] All systems were prepared with 2.39 g of L-α-phosphatidylcholine (PC), 1.40 g of dioctyl sulfosuccinate sodium salt (DOSS), 5 ml of hexadecane and 2.5 ml of water. $\alpha_{\text{Tween 80}}$, α_{PC}, α_{DOSS}, α_w and α_o represent the percentage weight fractions of Tween 80, PC, DOSS, all three amphiphiles, water (aqueous phase) and hexadecane (oil phase) respectively.

hydrophobic oil phase and the water [1,2]. The use of a PC-DOSS system (without Tween 80) marginally improves the emulsion stability, especially at a DOR of 1:20. In comparison, the PC-DOSS-Tween 80 system dramatically improves the stability with no increase in transmittance over 30 min, indicating that the oil droplets in the water column are stable to coalescence over this time period.

Fig. 3 shows optical microscopy images of the crude oil-in saline water emulsions prepared using the PC-DOSS system without Tween 80 (Fig. 3a–d) and with Tween 80 content of 27 wt% (Fig. 3e and f). Optical microscopy images of the emulsion prepared with the PC-DOSS system reveals that the interfacial film is unable to provide required resistance to droplet coalescence over relatively short times (Fig. 3a–d). Fig. 3e and f reveals the significant influence of introducing Tween 80 into the system on the resistance of the surfactant film at the crude oil-saline water interface to droplet coalescence. On addition of Tween 80 to PC and DOSS components, the surfactant film becomes effective in stabilizing the emulsion with the spherical shape and size of the droplets kept intact.

Fig. 4a shows optical microscopy images of crude oil-saline water emulsions prepared with systems having increasing Tween 80 content. Smaller droplet sizes are obtained with increasing Tween 80 content of the gel-like system, with average droplet sizes of 41.04 µm and 9.20 µm at Tween 80 content of 6 wt% and 27 wt% respectively. In addition, about 99% of the droplets are in the 0–25 µm range for the system having Tween 80 content of 27 wt% compared to 49% for the system with 6 wt% Tween 80 (Fig. 4b).

The interfacial tension curves in Fig. 5 reveal that increasing Tween 80 content of the dispersant system leads to a progressive decrease in crude oil-saline water interfacial tension at all the dispersant to oil ratios. Neglecting energy losses as heat through viscous dissipation or during mixing, the work input required (W) to disperse a liquid of volume V with drops of radius R in an immiscible liquid is [3]:

$$W = \gamma * \frac{3V}{R} \tag{3}$$

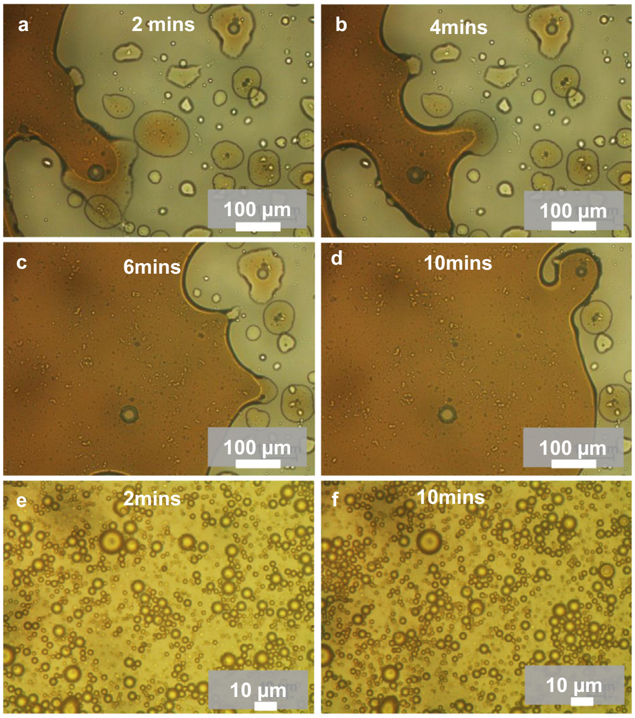

Fig. 3. (a–d) Instability of the interfacial surfactant film to droplet coalescence for O/W emulsions prepared using surfactant system containing PC and DOSS alone; (e and f) Influence of Tween 80 addition into surfactant system on the resistance of the surfactant film against droplet coalescence. Dispersant to oil mass ratio is 1:20 and oil to saline water ratio is 1:50.

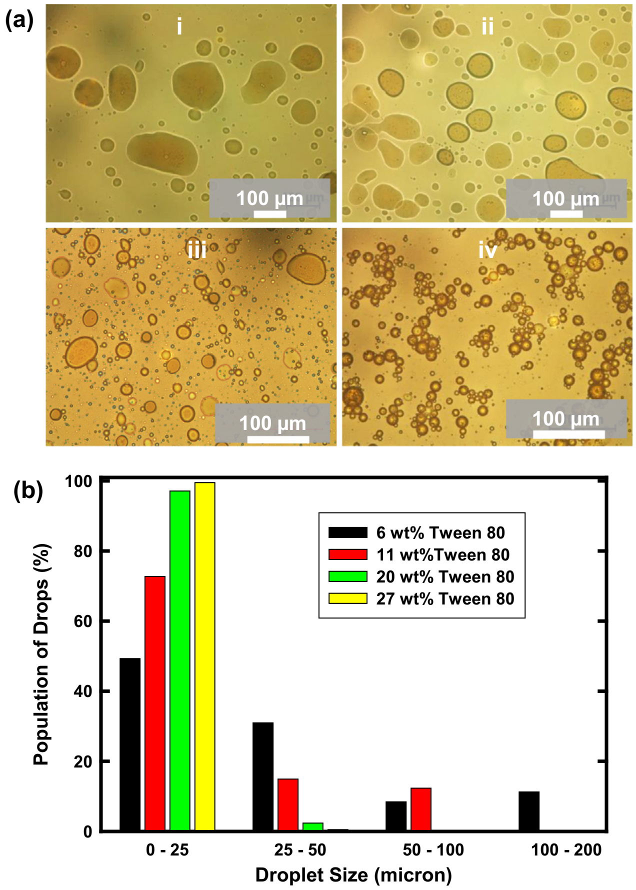

Fig. 4. Optical microscopy images (a) and droplet size distributions (b) of crude oil-in-saline water emulsions prepared with surfactant systems (dispersant) containing PC, DOSS and increasing amounts of Tween 80. Optical microscopy images were taken immediately after emulsion preparation. In Panel a, the Tween 80 content of the dispersants were 6 wt% (i), 11 wt% (ii), 20 wt% (iii) and 27 wt% (iv). Dispersant to oil mass ratio is 1:20 and oil to saline water ratio is 1:50.

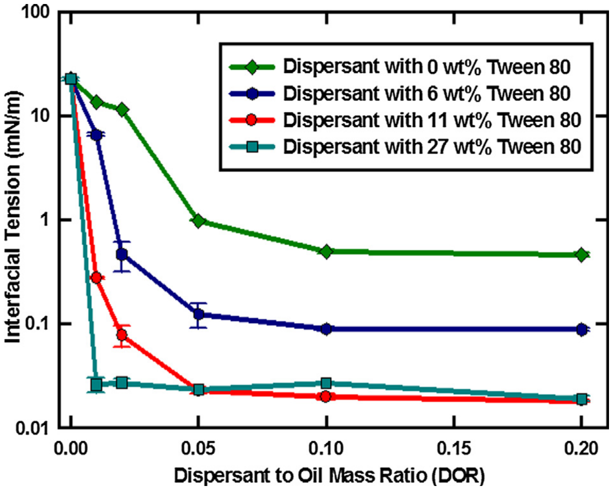

Fig. 5. Crude oil–saline water interfacial tension measured by the pendant drop and spinning drop techniques. The surfactant system serves as the gel-like dispersant.

where γ is the interfacial tension [17]. From Eq. (3), the effectiveness of oil emulsification is strongly dependent on the oil-water interfacial tension.

The impact of incorporating Tween 80 on interfacial tension reduction is more pronounced at the lower DORs (1:100 and 1:50), yielding more than two orders of magnitude reduction in the interfacial tension. This significant reduction in interfacial tension at small DOR's is a beneficial characteristic of the concentrated, gel-like system. Although the dispersant to oil ratio is an important parameter, the interfacial tension measurements reveal that the synergistic interactions of the surfactant components plays the major role in reducing the interfacial tension and stabilizing the crude oil-saline water interface.

Using Eq. (3), two systems 1 and 2 with constant work input (W) and liquid volumes (V) can be related by,

$$\frac{\gamma_1}{R_1} = \frac{\gamma_2}{R_2} \tag{4}$$

The emulsion prepared with the dispersant having 11 wt% Tween 80 has an average droplet size of 22.27 µm with a measured interfacial tension of 0.077 mN/m. Using Eq. (4), the decrease of interfacial tension to 0.027 mN/m for the dispersant having 27 wt% Tween 80 translates to a theoretical average droplet size decrease to 7.81 µm, close to the experimentally obtained average droplet size of 9.20 µm.

The surfactant components adsorb at the liquid-liquid interface to (i) reduce the interfacial tension and the thermodynamic instability of the system arising from the increase in the liquid-liquid interfacial area and (ii) provide a barrier to stabilize the dispersed droplets against coalescence [24] The reduction in interfacial tension facilitates oil emulsification into tiny droplets with minimal wave energy input, relevant to oil spill remediation applications. The formation and stabilization of a large oil-water interfacial area makes the oil droplets readily available food sources for naturally occurring microorganisms [6].

Fig. 6 shows the mechanism of oil dispersion by the gel-like surfactant system. Crude oil is first applied to the water surface followed by the addition of the surfactant system. Mixing energy was applied using a magnetic stirrer to facilitate breakdown of the gel and the emulsification of the surface oil layer. The side-view photograph in Fig. 6 v shows that the gel is positively buoyant on water. The gel anchors to the surface oil layer, breaks down on input of mixing energy and facilitates oil dispersion into droplets that are suspended in the water column.

The buoyancy of the gel-like dispersant can significantly enhance the encounter rates of the dispersant with floating crude oil layers on water [10]. Although phospholipid based gels may be prepared with a range of organic solvents several of which are biocompatible [25,26], the gel system with hexadecane as the organic solvent are solidified at cold temperatures below the phase transition temperature of hexadecane (18 °C) [27]. The solid nature of the gel dispersants in cold environment such as in arctic spills may further improve the oil-dispersant contact and prevent dispersant wastage.

3.2. Microstructure of Gel-like surfactant system

3.2.1. Small angle neutron scattering (SANS) analysis

Fig. 7 shows the neutron scattering curves of the gel-like surfactant mesophases as a function of Tween 80 content. The plots of scattering intensity, I(q), versus scattering vector (q) for all the systems show the presence of at least one strong peak indicative of a periodic structure [15]. Overall the q value of the peak is higher for the system prepared with PC and DOSS alone compared to all the systems containing Tween 80. This corresponds to an increased periodicity (d-spacing) on addition of Tween 80. The peak shifts from 0.081 Å^{-1} to lower q values of 0.072 Å^{-1} and 0.069 Å^{-1} for the systems with 6 wt% and 11 wt% Tween 80 respectively.

The q position of the scattering peak is inversely related to the spacing d by $q = 2\pi/d$ [28]. Thus, the peak shifts to lower q values on adding 6 wt% and 11 wt% of Tween 80 into the gel-like system corresponds to an increase in the characteristic repeat distance of about 10 Å and 13 Å respectively between aqueous domains. This observed "swelling" effect in the aqueous domain size at constant D_2O content may be due to the partitioning of the water soluble surfactant, Tween 80, with large headgroups between the bulk aqueous domains and the amphiphilic layer separating the aqueous and organic domains.

At a higher Tween 80 loading of 20 wt%, the peak shifts back to a higher q value of 0.074 Å^{-1}. Further increase of the Tween 80 content of the gel to 23 wt% and 27 wt% shifts the peak position to even higher values of 0.076 Å^{-1} and 0.078 Å^{-1} respectively. The reversal of the initial trend in which the peak shifts to low q values at the smaller Tween 80 loadings of 6 wt% and 11 wt%, suggests a significant structural transition. The hypothesis of a structure transition with increasing Tween 80 content of the gel system is corroborated by a progressive decrease in the intensity and decay characteristics of the scattering curves in the low q regime (<0.02 Å^{-1}).

To obtain quantitative structural information, the SANS data were fit by a sum of the power law and Teubner-Strey (TS) model functions using the sum model macro implemented in Igor Pro [29]. The scattering intensity $I(q)$ is fit by the equation [30,31]:

$$I(q) = Aq^{-m} + \frac{8\pi}{\xi}\left[\frac{\phi(1-\phi)(\Delta\rho)^2 c_2}{a_2 + c_1 q^2 + c_2 q^4}\right] \tag{5}$$

where q is the scattering vector, ξ is the correlation length, ϕ is the volume fraction of the deuterated component; $\Delta\rho$ is the scattering contrast and A, m, a_2, c_1, c_2 are model coefficients. The power law model describes the scattering intensity simply in terms of the decay exponent (m) and coefficient (A). The power law model function accounts for the decay in scattering intensity in the low q regime (<0.02 Å^{-1}) and the TS model function models the scattering peak of structured two-phase systems [30].

Fig. 7 shows that the SANS data is well fit by the summed model. We note that the summed model is an approximation of the scattering spectra. However, the summation of the model functions allows the extraction of detailed structural information from the scattering profiles and this approach has been used to characterize structured two-phase systems [31,32]. The correlation length is the length scale over which periodicity remains and is a measure of the long range order in a system or the dispersion in the periodicity. The periodicity (d) relates to the mean repeat distance between alternating water and oil (hexadecane) domains. An amphiphilicity factor (f_a), calculated from the model coefficients, provides a quantitative measure of the strength of the surfactant components to impart order on a system where f_a value of 1.0 corresponds to a disordered system and f_a values close to −1.0 indicates an ordered lamellar phase [33].

The periodic repeat distance (d), correlation length (ξ) and amphiphilicity factor (f_a) are related to the model coefficients by [30]:

$$d = 2\pi\left[\frac{1}{2}\left(\frac{a_2}{c_2}\right)^{1/2} - \left(\frac{c_1}{4c_2}\right)\right]^{-1/2} \tag{6}$$

$$\xi = \left[\frac{1}{2}\left(\frac{a_2}{c_2}\right)^{1/2} + \left(\frac{c_1}{4c_2}\right)\right]^{-1/2} \tag{7}$$

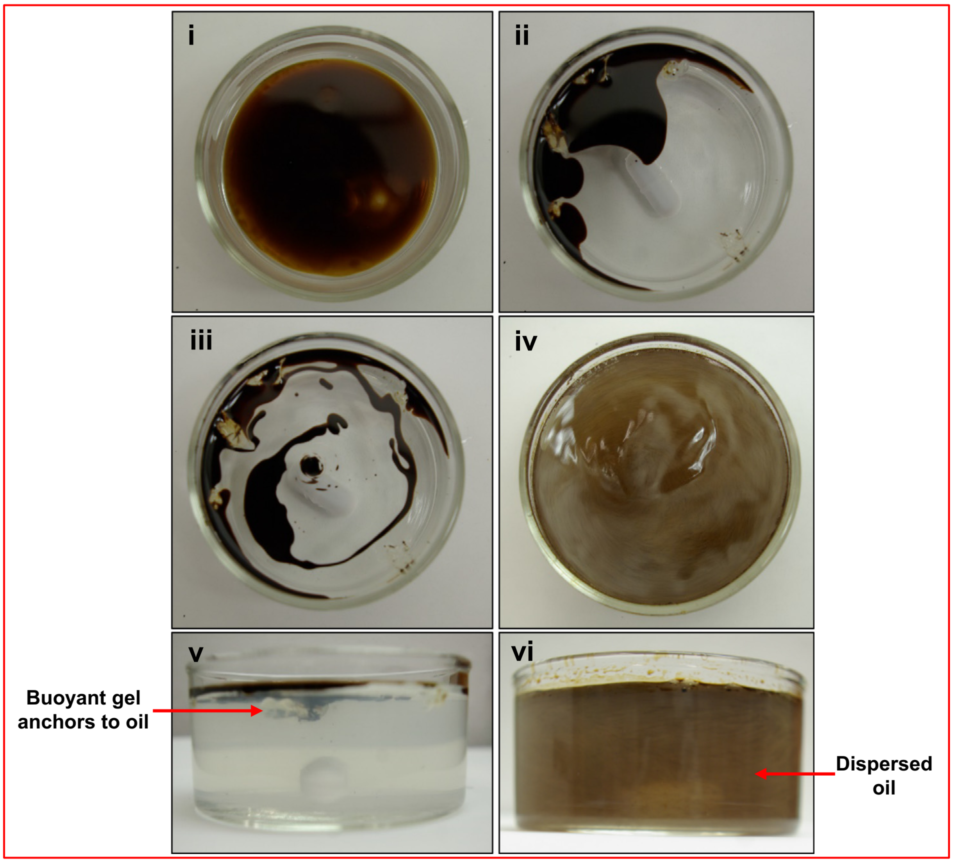

Fig. 6. Surface oil dispersion using gel-like surfactant system. Gel-like system contains PC, DOSS and Tween 80. Tween 80 content is 27 wt%. (i) Oil is added to water surface (ii) Surfactant system (gel-like dispersant) is added to oil layer (iii) the system is mixed gently with a stirrer (iv) The oil is dispersed on input of sufficient mixing energy (v) Side-view of photograph in iii (vi) Side-view of photograph in iv.

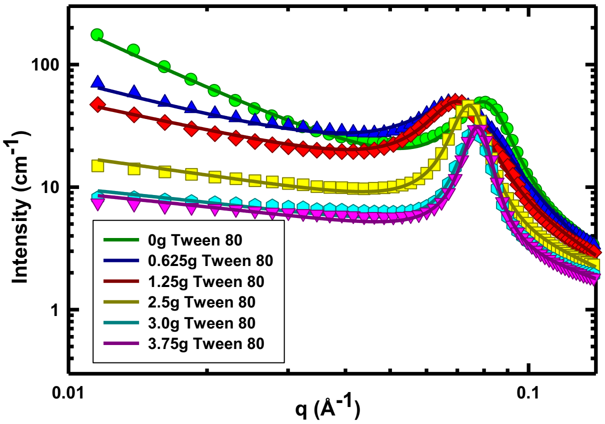

Fig. 7. SANS data on a on a log-log scale for surfactant systems containing varying amounts of Tween 80 analyzed at 25 °C The solid lines are the model fits while the symbols are the experimental scattering data points at 25 °C. The parameters for each fit are listed in Table 3. All systems were prepared with equimolar amounts of DOSS and PC in hexadecane.

$$f_a = \frac{c_1}{\sqrt{4a_2c_2}} \tag{8}$$

Initial input parameters for the summed model were obtained by fitting the low q regime (<0.020 Å^{-1}) and the q range around the peak (0.055 Å^{-1}–0.140 Å^{-1}) separately by the power law and TS model functions respectively. The obtained values from the initial fits are good estimates of the input parameters for the summed model, facilitating the fast and accurate model fitting of the SANS data (Fig. 7).

Table 3 lists the fit parameters obtained for the SANS data. The model fits shows a low q power-law behavior with exponents (m) of 1.71, 1.02, and 0.81 for systems containing 0 wt%, 6 wt% and 11 wt% of Tween 80 respectively. At high Tween 80 loadings of 23 wt% and 27 wt%, the magnitude of the low q slope plateaus to smaller values of 0.21 and 0.19 respectively on a log-log scale. The low q region below the interaction peak can be considered as the Porod region of larger length scale structures or quasi periodically ordered domains in the surfactant system. The progressive decrease of the low q slope suggests that the size of the quasi periodic domains increases with Tween 80 content until beyond the length scale of SANS measurement.

The periodicity is higher for the systems containing Tween 80 compared to the system with PC and DOSS alone (Table 3) in agreement with the peak shift to lower q values. At Tween 80 loadings of 20 wt% and above, the SANS data fitting reveals a significant increase in correlation length. The correlation length at Tween 80 loading of 27 wt% is 212.15 Å, more than double the correlation length of 91.55 Å for the system without Tween 80. The addition of Tween 80 significantly increases the length scale over which the quasi periodical order of the system is retained. The sharpening of the peak with addition of Tween 80 (Fig. 7) also indicates a more well-defined repeat distance compared to the system with PC and DOSS alone. The closeness of the amphiphilicity factors to −1.0 for ordered lamellar morphologies [33] shows that the amphiphiles act synergistically to impose a high degree of order.

3.2.2. ^{31}P nuclear magnetic resonance (NMR) spectroscopic analysis

^{31}P NMR provides a specific probe of the structure and molecular interactions as the system contains only a single phosphorus

Table 3
Fit parameters for the SANS data of the gel-like surfactant system.

Tween 80 in Gel (wt %)	Low q power law exponent (m)	Low q power law coefficient (A)	Periodicity d (Å)	Correlation length ξ (Å)	Amphiphilicity factor (f_a)
0	−1.71	0.08	78.03	91.55	−0.96
6	−1.02	0.62	87.59	62.00	−0.90
11	−0.81	1.19	88.54	93.71	−0.96
20	−0.41	3.36	84.40	170.98	−0.99
23	−0.21	6.70	82.05	192.68	−0.99
27	−0.19	7.30	80.87	212.15	−0.99

atom from the PC [16]. The ^{31}P nucleus has an electron shell that is not spherically symmetric [16]. Thus, the ^{31}P chemical shift is a tensor and depends on the orientation of the phosphorus group with respect to the external magnetic field [16,34]. In the ^{31}P NMR, the restricted motion of the phosphorus containing PC molecules in viscous anisotropic assembly results in chemical shift anisotropy that reveals the phase characteristics and local environment of the ^{31}P nucleus [16,34].

The value of the chemical shift anisotropy ($\Delta\sigma$) from the superposition of chemical shifts in various orientations relative to the magnetic field is given by [16,34]:

$$\Delta\sigma = \sigma_{11} - (\sigma_{22} + \sigma_{33})/2 = \sigma_{\parallel} - \sigma_{\perp} \tag{9}$$

where σ_{11}, σ_{22}, and σ_{33} are chemical shifts along three principal directions with σ_{11} defined as the unique axis. The chemical shift σ_{11} corresponds to the chemical shift when the magnetic field is parallel to the unique axis ($\sigma_{\parallel}$) while the average of σ_{22} and σ_{33} is defined as the chemical shift when the unique axis is perpendicular to the magnetic field ($\sigma_{\perp}$) [16,34].

The NMR spectra for the PC-DOSS system without Tween 80 in Fig. 8 exhibits an upfield peak ($\sigma_{\perp}$) at −11.72 ppm and a long downfield tail ($\sigma_{\parallel}$) at ~12.00 ppm, a typical signature of a lipid lamellar structure [16,34,35]. The NMR spectrum exhibits a weak shoulder at about −1.0 ppm indicative that some surfactant may be present in an isotropic phase [16]. Using Eq. (9), the ^{31}P chemical shift anisotropy of the lamellar phase is calculated to be ~23.72 ppm. The gels with Tween 80 content of 11 wt% and 27 wt% also show the upfield peak and long downfield tail characteristics, indicative of lamellar phase morphology [16,34,35]. The upfield peaks are sharpened on introduction of Tween 80 to the gel system. The weak isotropic peak disappears on the addition of Tween 80, indicating that the gel system transitions into a more ordered lamellar phase. This is in agreement with the increase in the degree of order in the system from the SANS analysis and modelling. The upfield peak ($\sigma_{\perp}$) has a chemical shift of −11.72 ppm, −11.53 ppm and −11.05 ppm at Tween 80 loadings of 0 wt%, 11 wt% and 27 wt% respectively. The progressive shift of the peak ($\sigma_{\perp}$) downfield with increasing Tween 80 content suggests that the addition of Tween 80 deshields the phosphorus nucleus and alters the local environment around the PC phospholipid.

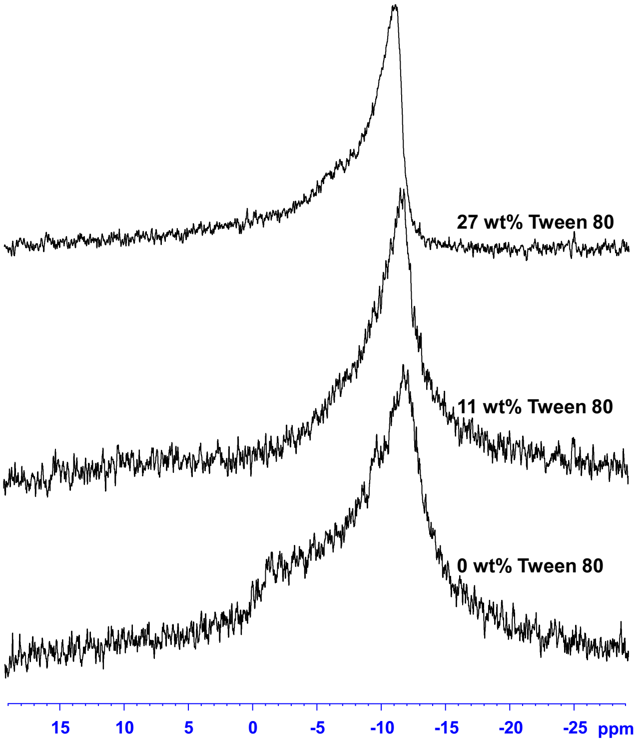

Fig. 8. ^{31}P NMR spectra of PC-DOSS-Tween 80 gel systems measured at 25 °C. The weight percent of Tween 80 in the gels are 0 wt%, 11 wt% and 27 wt% respectively.

3.2.3. Cryogenic scanning electron microscopy (cryo-SEM) imaging

Cryo-SEM imaging allows a direct microscopic visualization of the microstructure in the gel-like surfactant system (Fig. 9). Fig. 9a and b shows the lamellar phase morphology of the gel prepared with PC and DOSS alone. The overall lamellar microstructure is still observed in the gel-like system with 11 wt% of Tween 80 (Fig. 9c, d). The lamellar phase shows some undulation on addition of 11 wt% of Tween 80 compared to the relatively straight, lamellar morphology without Tween 80. The quasi periodic lamellar structures are about 100–200 nm in diameter and span length scales of up to 2 μm (Fig. 9a–d). At a repeat distance of 78.029 Å for the gel-like system with PC and DOSS (Table 3), the number of unit cells across a 100–200 nm quasi periodic domain is calculated to range from about 12 to 24.

Cryo-SEM images of the gel incorporating a higher Tween 80 loading of 27 wt% shows discrete spherical structures (Fig. 9e–h), corroborating the structural transition observed in the SANS and NMR spectroscopic analysis. The spherical domains range from about 1 μm–5 μm. Cryo-SEM imaging reveals that the transition is likely due to the rolling of long, flexible and closely-packed lamellar assemblies into onion-like multilamellar structures at high Tween 80 loading (Fig. 9e, f). Cryo-SEM imaging allows the visual distinction between the straight lamellar and curved multilamellar structures compared to the scattering (SANS) and spectroscopic (NMR) analysis.

The microstructural transition on addition of Tween 80 may be rationalized in molecular terms as a consequence of the change in the average packing parameter [1] of the surfactant mixture. The equilibrium structure of surfactant aggregates and the spontaneous interfacial curvature is described in terms of a molecular packing parameter ($P = v/al$) where v is the volume occupied by the surfactant tails, a is the effective headgroup cross-sectional area and l is the maximum effective tail length [1]. DOSS has a surfactant packing parameter (P) of 1.1, spontaneously adopting a concave curvature towards water resulting in the formation of spherical reversed micelles above the cmc [15]. The phospholipid, PC has a packing parameter of 0.6 and tends to form assemblies such as wormlike reverse micelles in non-polar solvents with interfaces of minimal curvatures [15]. The packing parameter of Tween 80 is about 0.07 [36] due to the relatively large headgroup and short tail features. Surfactant with packing parameters ≤0.33

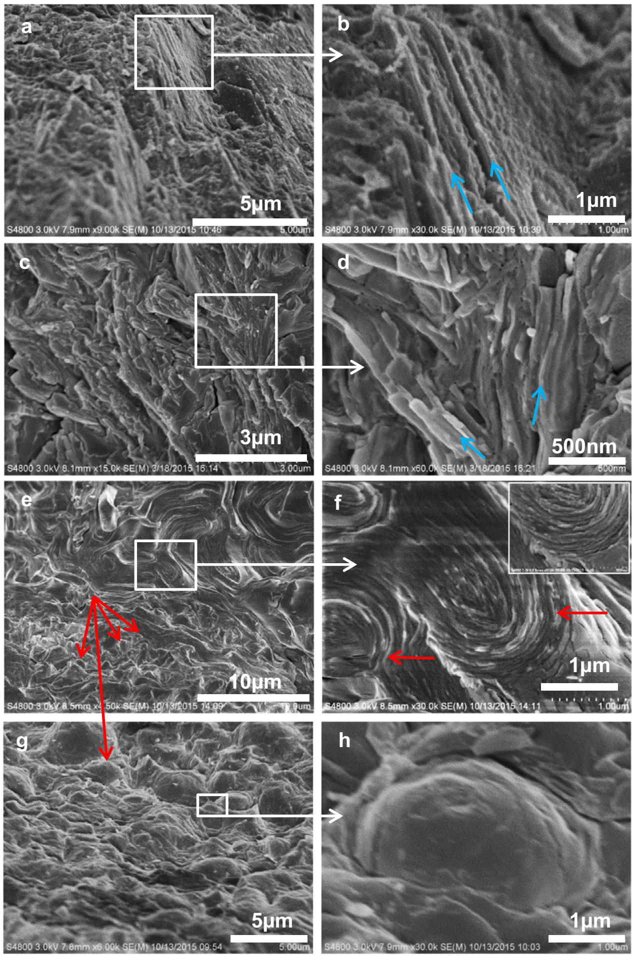

Fig. 9. Representative cryo-scanning electron microscopy images of PC-DOSS gel system with increasing Tween 80 loadings of 0 wt% (a,b), 11 wt% (c,d) and 27 wt% (e–h). All gels were prepared with equimolar amounts of DOSS and PC in hexadecane. The lamellar and onion-like multilamellar structures are indicated by the blue and red arrows in Fig. 9a–d and Fig. 9e–h respectively.

favorably form aggregates such as micelles with spherical curvatures [3,36].

Mixtures of amphiphilic molecules with different packing parameters may be described in terms of a mean packing parameter ($P_{mixture} = \Sigma n_i P_i$) where n_i and P_i are the mole fraction and packing parameter of the individual surfactant in the mixture respectively [1,37]. The gel-like system prepared with equimolar concentrations of PC and DOSS has a calculated $P_{mixture}$ of 0.85. On incorporation of increasing amounts of Tween 80; 6 wt%, 11 wt%, 20 wt% and 27 wt%; the P_{mix} values are calculated to be 0.80, 0.75, 0.67, and 0.61 respectively. The incorporation of Tween 80 into the PC/DOSS gel system alters the packing characteristics to favor more spherical (curved) geometries. This may explain the transition from straight lamellae to spherical, multilamellar structures.

3.2.4. Rheological characterization

The dynamic rheological response of the gel-like surfactant mesophase with and without Tween 80 is presented in Fig. 10. Both samples show the characteristic response of an elastic gel. That is, the storage or elastic modulus (G′) is greater than the loss or viscous modulus (G″) over the range of frequencies, and both moduli are nearly independent of frequency. These features are consistent with the surfactant assemblies forming a close-packed network that spans the sample. This network is able to store the imposed deformation energy, which explains why the moduli do not relax at low frequencies (long time scales). Surprisingly, the presence of Tween 80 has negligible influence on the value of the elastic modulus, even though the structure in the gel is altered significantly by the Tween 80. The same samples show a yield stress and a shear-thinning response when examined under steady-shear rheology (data not shown).

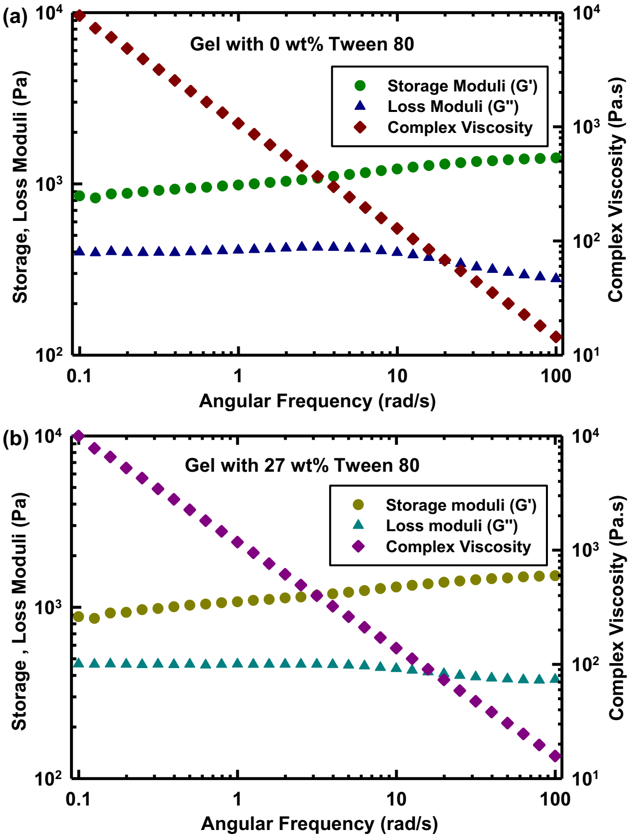

Fig. 10. Storage (*G*′), loss moduli (*G*″) and complex viscosity as a function of angular frequency at T = 25 °C. The angular frequency range was 0.1–100 rad/s and the strain was kept constant at 0.5%.

4. Conclusions

In the treatment of marine oil spills, gel-like dispersants have inherent advantages over traditional liquid dispersants including buoyancy for extended periods, improved adherence to the spill oils in the presence of ocean current, higher surfactant concentrations and provision of visible feedback to oil spill responders [10]. A gel-like surfactant mesophase containing surfactant components of Corexit dispersants (DOSS, Tween 80) [8,19] and a widely available double-tailed phospholipid, PC, as zwitterionic surfactant has been developed for oil spill remediation. The gel-like phase is formed on addition of water to a micellar solution of PC and DOSS in an organic solvent. The combination of PC and DOSS is necessary to form the gel-like system. The introduction of Tween 80 into the gel-like system significantly imparts the ability of the surfactant system to stabilize crude oil-in-saline water emulsions. The combination of Tween 80 with DOSS and PC lowers the crude oil-saline water interfacial to the 10^{-2} mN/m range, a level appropriate for the dispersion of spill oils into small droplets [5,7,38]. The surfactant mixture in the gel-like system disperses crude oil layers into small droplets that are stable for extended periods. The structural integrity of the gel-like surfactant system imparts buoyancy characteristics on water, leading to potential applications as a buoyant dispersant for oil spill remediation. The structural order of the system produces very clear neutron scattering peaks. Increasing loading of Tween 80 leads to a structural transition from a gel-like mesophase consisting of lamellar to spherical, onion-like multilamellar structures accompanied by a significant increase in the correlation length of the gel microstructure. Cryo-SEM imaging allowed the direct visualization of the rolling of the sheet-like lamellar structures into spherical multilamellar structures. Aspects of continuing work include preparing the gel-like surfactant system using food-grade oils and characterizing the dispersion effectiveness on oils spanning a wide range of viscosities using the baffled flask test [39,40]. Spatial compartmentalization of nanoparticles in the gel-like surfactant system or encapsulation of the gels within the tubular void volume of interfacially-adherent clay nanotubes can provide a unique approach to design mixed surfactant and particle emulsifier systems [7,41–43].

Acknowledgements

This research was made possible in part by a grant from The Gulf of Mexico Research Initiative. The Small Angle Neutron Scattering (SANS) for this project was supported by the U.S. Department of Energy (DOE) under EPSCOR Grant No. DE-SC0012432 with additional support from the Louisiana Board of Regents. Data are publicly available through the Gulf of Mexico Research Initiative Information & Data Cooperative (GRIIDC) at https://data.gulfresearchinitiative.org (doi: 10.7266/N7KP80N4).

Appendix A. Supplementary material

Supplementary data associated with this article can be found, in the online version, at https://doi.org/10.1016/j.jcis.2018.03.089.

References

[1] 1. Israelachvili, J. N. Intermolecular and Surface Forces; 3rd ed.; Elsevier: London, 2010

[2] M.J. Rosen, Surfactants and Interfacial Phenomena, 3rd ed., John Wiley & Sons, Hoboken, NJ, 2004.

[3] F. Evans, H. Wennerstrom, The Colloidal Domain: Where Physics, Chemistry, Biology, and Technology Meet, Wiley VCH New York, NY, 1999.

[4] S.M. Kirby, S.L. Anna, L.M. Walker, Sequential adsorption of an irreversibly adsorbed nonionic surfactant and an anionic surfactant at an oil/aqueous interface, Langmuir 31 (14) (2015) 4063–4071.

[5] M. Fingas, Oil Spill Science and Technology, Gulf Professional Publishing, Boston, 2011.

[6] R.C. Prince, Oil spill dispersants: boon or bane?, Environ Sci. Technol. 49 (11) (2015) 6376–6384.

[7] O. Owoseni, E. Nyankson, Y.H. Zhang, S.J. Adams, J.B. He, G.L. McPherson, A. Bose, R.B. Gupta, V.T. John, Release of surfactant cargo from interfacially-active halloysite clay nanotubes for oil spill remediation, Langmuir 30 (45) (2014) 13533–13541.

[8] D.A. Riehm, A.V. McCormick, The role of dispersants' dynamic interfacial tension in effective crude oil spill dispersion, Marine Pollut. Bullet. 84 (1–2) (2014) 155–163.

[9] C.P.E. Brochu, G. Caron, J.E. Desnoyers, Dispersion of crude oil in seawater: The role of synthetic surfactants. Oil and Chemical Pollution (1986) 3, 257–279.

[10] T. Nedwed, G.P. Canevari, J.R. Clark, R. Belore, In New dispersant delivered as a gel, International Oil Spill Conference, 2005; American Petroleum Institute: Washington, DC, pp 121–125.

[11] E. Nyankson, C.A. Ober, M.J. DeCuir, R.B. Gupta, Comparison of the effectiveness of solid and solubilized dioctyl sodium sulfosuccinate (DOSS) on Oil dispersion using the baffled flask test, for crude oil spill applications, Ind. Eng. Chem. Res. 53 (29) (2014) 11862–11872.

[12] J.C. Athas, K. Jun, C. McCafferty, O. Owoseni, V.T. John, S.R. Raghavan, An effective dispersant for oil spills based on food-grade amphiphiles, Langmuir 30 (31) (2014) 9285–9294.

[13] E. Nyankson, M.J. DeCuir, R.B. Gupta, Soybean lecithin as a dispersant for crude oil spills, Acs. Sustain. Chem. Eng. 3 (5) (2015) 920–931.

[14] G.L. Pi, L.L. Mao, M.T. Bao, Y.M. Li, H.Y. Gong, J.R. Zhangt, Preparation of oil-in-seawater emulsions based on environmentally benign nanoparticles and biosurfactant for oil spill remediation, Acs. Sustain. Chem. Eng. 3 (11) (2015) 2686–2693.

[15] B.A. Simmons, G.C. Irvin, V. Agarwal, A. Bose, V.T. John, G.L. McPherson, N.P. Balsara, Small angle neutron scattering study of microstructural transitions in a surfactant-based gel mesophase, Langmuir 18 (3) (2002) 624–632.

[16] L. Liu, G. Tan, G. McPherson, V.T. John, K. Maskos, A. Bose, High-resolution NMR characterization of a gel-like surfactant mesophase, Langmuir 24 (17) (2008) 9286–9294.

[17] G. Tan, P. Xu, V.T. John, J. He, G.L. McPherson, V. Agarwal, A. Bose, Cryo-field emission scanning electron microscopy imaging of a rigid surfactant mesophase, Langmuir 24 (19) (2008) 10621–10624.

[18] A. Zattoni, E.L. Piccolomini, G. Torsi, P. Reschiglian, Turbidimetric detection method in flow-assisted separation of dispersed samples, Analyt. Chem. 75 (23) (2003) 6469–6477.

[19] P. Venkataraman, J.J. Tang, E. Frenkel, G.L. McPherson, J.B. He, S.R. Raghavan, V. Kolesnichenko, A. Bose, V.T. John, Attachment of a hydrophobically modified biopolymer at the oil-water interface in the treatment of oil spills, Acs. Appl. Mater. Inter 5 (9) (2013) 3572–3580.

[20] B. Vonnegut, Rotating bubble method for the determination of surface and interfacial tensions, Rev. Sci. Instruments 13 (1942) 6–9.

[21] J.W. Goodwin, Colloids and Interfaces with Surfactants and Polymers—An Introduction, John Wiley & Sons Ltd, New York, 2004.

[22] O. Arnold, J.C. Bilheux, J.M. Borreguero, A. Buts, S.I. Campbell, L. Chapon, M. Doucet, N. Draper, R.F. Leal, M.A. Gigg, V.E. Lynch, A. Markyardsen, D.J. Mikkelson, R.L. Mikkelson, R. Miller, K. Palmen, P. Parker, G. Passos, T.G. Perring, P.F. Peterson, S. Ren, M.A. Reuter, A.T. Savici, J.W. Taylor, R.J. Taylor, R. Tolchenoy, W. Zhou, J. Zikoysky, Mantid-Data analysis and visualization package for neutron scattering and mu SR experiments, Nucl. Instrument. Methods Phys. Res. Section a-Accelerat. Spectrometers Detect. Associat. Equip. 764 (2014) 156–166.

[23] G.D. Wignall, F.S. Bates, Absolute calibration of small-angle neutron-scattering data, J. Appl. Crystallograph. 20 (1987) 28–40.

[24] M. Fingas, Oil Spill Science and Technology. Gulf Professional Publishing: Boston, MA, 2011; p 444.

[25] R. Angelico, A. Ceglie, G. Colafemmina, F. Lopez, S. Murgia, U. Olsson, G. Palazzo, Biocompatible lecithin organogels: structure and phase equilibria, Langmuir 21 (1) (2005) 140–148.

[26] R. Scartazzini, P.L. Luisi, Organogels from lecithins, J. Phys. Chem. 92 (3) (1988) 829–833.

[27] R.T.Zheng, J.W. Gao, J.J. Wang, G. Chen, Reversible temperature regulation of electrical and thermal conductivity using liquid-solid phase transitions, Nature Communications 2011, 2. 0–0

[28] J.S. Higgins, H.C. Benoit, Polymers and Neutron Scattering, Oxford University Press, 1994.

[29] S.R. Kline, Reduction and analysis of SANS and USANS data using IGOR Pro, J Appl Crystallogr 39 (2006) 895–900.

[30] M. Teubner, R. Strey, Origin of the scattering peak in microemulsions, J. Chem. Phys. 87 (5) (1987) 3195–3200.

[31] M. Laupheimer, T. Sottmann, R. Schweins, C. Stubenrauch, Studying orthogonal self-assembled systems: microstructure of gelled bicontinuous microemulsions, Soft Matter. 10 (43) (2014) 8744–8757.

[32] P.J. Atkinson, B.H. Robinson, A.M. Howe, R.K. Heenan, Structure and stability of microemulsion-based organogels, J. Chem. Soc. Faraday Trans. 87 (1991) 3389–3397.

[33] K.V. Schubert, R. Strey, S.R. Kline, E.W. Kaler, Small-angle neutron-scattering near lifshitz lines - transition from weakly structured mixtures to microemulsions, J. Chem. Phys. 101 (6) (1994) 5343–5355.

[34] D. Gorenstein, Phosphorus-31 NMR: Principles and Applications, Academic Press, New York, 1984.

[35] R.L. Thurmond, G. Lindblom, M.F. Brown, Curvature, order, and dynamics of lipid hexagonal phases studied by deuterium nmr-spectroscopy, Biochemistry 32 (20) (1993) 5394–5410.

[36] A. Amani, P. York, H. de Waard, J. Anwar, Molecular dynamics simulation of a polysorbate 80 micelle in water, Soft Matter. 7 (6) (2011) 2900–2908.

[37] C. Manohar, J. Narayanan, Average packing factor approach for designing micelles, vesicles and gel phases in mixed surfactant systems, Colloids Surfaces a-Physicochem. Eng. Aspects 403 (2012) 129–132.

[38] J.C. Athas, K. Jun, C. McCafferty, O. Owoseni, V.T. John, S.R. Raghavan, An effective dispersant for oil spills based on food-grade amphiphiles, Langmuir (2014).

[39] A.D. Venosa, D.W. King, G.A. Sorial, The baffled flask test for dispersant effectiveness: a round robin evaluation of reproducibility and repeatability, Spill Sci. Technol. B 7 (5–6) (2002) 299–308.

[40] E. Nyankson, O. Olasehinde, V.T. John, R.B. Gupta, Surfactant-loaded halloysite clay nanotube dispersants for crude oil spill remediation, Ind. Eng. Chem. Res. 54 (38) (2015) 9328–9341.

[41] O. Owoseni, E. Nyankson, Y. Zhang, D.J. Adams, J. He, L. Spinu, G.L. McPherson, A. Bose, R.B. Gupta, V.T. John, Interfacial adsorption and surfactant release characteristics of magnetically functionalized halloysite nanotubes for responsive emulsions, J. Colloid Interface Sci. 463 (2015) 288–298.

[42] O. Owoseni, Y. Zhang, Y. Su, J. He, G.L. McPherson, A. Bose, V.T. John, Tuning the wettability of halloysite clay nanotubes by surface carbonization for optimal emulsion stabilization, Langmuir (2015).

[43] R. Pichot, F. Spyropoulos, I.T. Norton, Mixed-emulsifier stabilised emulsions: Investigation of the effect of monoolein and hydrophilic silica particle mixtures on the stability against coalescence, J. Colloid Interface Sci. 329 (2) (2009) 284–291.

Supplementary material

Chemical structures of PC, DOSS and Tween 80

L-α-phosphatidylcholine (PC)

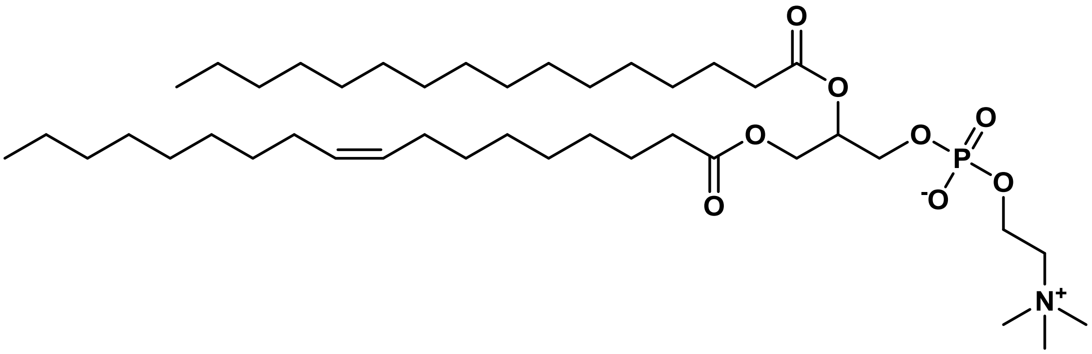

Dioctyl sulfosuccinate sodium salt (DOSS)

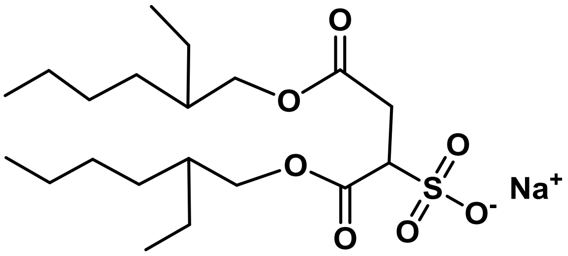

Polyoxyethylene (20) sorbitan monooleate (Tween 80)